Refined Edge Usage of Graph Neural Networks for Edge Prediction

Jiarui Jin[1], Yangkun Wang[2], Weinan Zhang[1], Quan Gan[3], Xiang Song[3], Yong Yu[1], Zheng Zhang[3], David Wipf[3].
[1]Shanghai Jiao Tong University, [2]University of California San Diego, [3]Amazon Web Service
{jinjiarui97,wnzhang,yyu}@sjtu.edu.cn,yaw048@ucsd.edu,{quagan,xiangsx,zhaz,daviwipf}@amazon.com

ABSTRACT

Graph Neural Networks (GNNs), originally proposed for node classification, have also motivated many recent works on edge prediction (a.k.a., link prediction). However, existing methods lack of elaborate design regarding the distinctions between two tasks that have been frequently overlooked: (i) edges only constitute *the topology* in the node classification task but can be used as both *the topology and the supervisions* (i.e., labels) in the edge prediction task; (ii) the node classification makes prediction over each *individual node*, while the edge prediction is determinated by each *pair of nodes*. To this end, we propose a novel edge prediction paradigm named Edge-aware Message PassIng neuRal nEtworks (EMPIRE). Concretely, we first introduce an edge splitting technique to specify use of each edge where each edge is solely used as either the topology or the supervision (named as topology edge or supervision edge). We then develop a new message passing mechanism that generates the messages to source nodes (through topology edges) being aware of target nodes (through supervision edges). In order to emphasize the differences between pairs connected by supervision edges and pairs unconnected, we further weight the messages to highlight the relative ones that can reflect the differences. In addition, we design a novel negative node-pair sampling trick that efficiently samples "hard" negative instances in the supervision instances, and can significantly improve the performance. Experimental results verify that the proposed method can significantly outperform existing state-of-the-art models regarding the edge prediction task on multiple homogeneous and heterogeneous graph datasets.

KEYWORDS

Edge-aware Message Passing; Edge Prediction; Edge Usage

1 INTRODUCTION

Graphs (e.g., social networks) as a common structure for complex relational data, have been recently involved in various machine learning tasks and received increasing attention. Among these tasks, node classification is one of the most prominent examples. Due to the remarkable success of graph convolution networks (GCNs) [11], many advanced graph neural networks (GNNs) (e.g., graph attention networks (GAT) [22], SAGE (so called GraphSAGE) [5]) designs have been proposed regarding the node classification problem.

Most of prevailing solutions of the edge prediction task are developed based on GNNs. These methods usually are directly extended from existing GNN frameworks by plugging the representation vectors of node pairs into a pre-defined scoring function. Unfortunately, there are significant differences between node classification task and edge prediction task, which are overlooked, or even not aware of, by these methods. Here, we summarize two main differences:

First, given a graph, for the node classification task, the supervisions (i.e., labels) are on the nodes, while the topology (i.e., graph structure) is free of the supervision and thus remains the same (and complete) during both training and test phrases. In contrast, for the edge prediction task, the supervisions are on the node pairs, and thus the edges are used both as the topology and the supervisions. Therefore, if directly applying the GNN models to the edge prediction task, it would simultaneously use the edges as both the topology and supervisions (i.e., using the whole graph as input and outputting the predictions over all the edges in the graph). We argue that this setting is problematic, as it would allow the model to observe the existence (i.e., the ground-truth) of the edges to predict, namely the labels are (indirectly) fed into the model during training. As a consequence, the GNN models are likely to *over-fit the training graph*, resulting in the low generalizability to the test graph.

Second, the classification of each node is solely determinated by the properties of the node; while the prediction over each edge depends on the properties of the node pair. We note that conventional message passing mechanisms, originally proposed for the node classification, are designed to aggregate the neighborhood of individual nodes. In this regard, directly applying them to the edge prediction task would make *the messages passing to the source nodes invariant to the target nodes*. In other words, the message generation is invariant to the edges to predict.

In this paper, we propose a novel edge prediction paradigm called Edge-aware Message PassIng neuRal nEtworks (EMPIRE), which tailors the message passing mechanism introduced in [4] regarding the aforementioned differences to make it a good fit for the edge prediction task.

To achieve this, we first refine the usage of the edges in the graph by splitting edges into two subsets: topology and supervision edges. The former and latter ones are used as topology and supervisions respectively at each split (as illustrated in Figure 1). For each round, we randomly sample the same number of unconnected node pairs as the negative supervision instances. Then, given the topology edges, our edge prediction models are trained by recovering the existences of those supervision edges.

Conference'23, Date, Location

ACM ISBN 978-x-xxxx-xxxx-x/YY/MM…$15.00
https://doi.org/10.1145/nnnnnnn.nnnnnnn

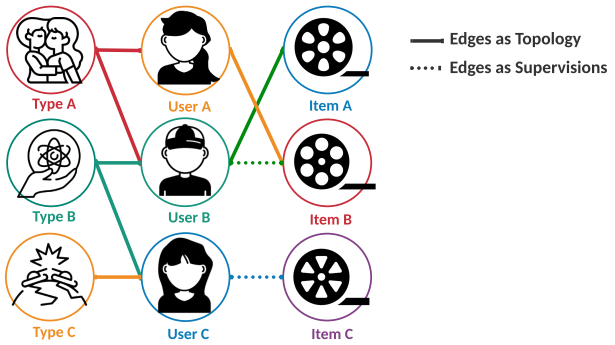

Figure 1: An illustrated example of the motivation of our target-aware message passing mechanism: (i) message from the neighbor node `Type C` to the source node `User C` should be weighted by the target node `Item C`; (ii) information that can distinguish node pair connected by supervision edges ⟨`User B`, `Item B`⟩ and unconnected node pair ⟨`User B`, `Item C`⟩ should be highlighted in the message passing to source node `User B`.

On the basis of the splitted edges, we argue that it is essential to make the messages to source nodes (through topology edges) being aware of target nodes (through supervision edges). Take Figure 1 as an example. Suppose `Item C` is a fiction movie, then when predicting the edge existence between `User C` and `Item C`, the message from `Type C` to `User C` should be highly weighted. In the light of this, we design to use target nodes to attend the messages to source nodes.

We also notice that after each split, there are three types of node pairs: ones connected by the topology edges, ones connected by the supervision edges, and unconnected ones; and obviously the likelihoods of the edge existence over these three types are different and listed in the descending order. Taking Figure 1 as an example, `User B` favors `Item A`, and is likely to favor `Item B`, but is unlikely to favor `Item C`. Hence, when passing the message from `Type A` and `Type B` to `User B`, we expect it to highlight the differences between `Item B` and `Item C`. For instance, if `Item B` is a romantic movie and `Item C` is a war movie, then we need to assign more attention on the message from `Type A` than `Type B`. To this end, we propose to highlight the relative messages that can reflect the differences between node pairs connected by supervision edges and unconnected node pairs.

In addition, we notice that the negative instances in the supervision instances play an important role in the final edge prediction, as they can significantly influence our message generation. Inspired by [35] which reveals that "hard" negative samples would improve the effectiveness and stability of the information retrieval models, we regard the unconnected node pairs satisfying the common-neighbor heuristics as "hard" negative samples in the edge prediction task. The underlying reason is that as the non-parametric common neighbor method [2] is a strong baseline regarding the edge prediction task, it would be hard to distinguish unconnected node pairs with the common neighbors and connected node pairs. However, as discussed in [19], finding all these node pairs is much time-consuming. To address this issue, we propose a new negative node-pair sampling trick, which allows us to efficiently sample/retrieve these node pairs as the negative samples.

In summary, the contributions of this paper are three-fold:

- We reveal that edges simultaneously used as topology and supervisions would encourage GNN models to over-fit the inputted training graph, and thus hold low generalizability to test graph.
- We develop an edge splitting technique and design a novel target-aware message passing mechanism based on the splitted edges to make messages conditioned on the source-target node pairs.
- We present a new negative node-pair sampling trick that efficiently samples "hard" node pairs satisfying the common-neighbor heuristics to construct the supervision edges.

Our empirical evaluation demonstrates that EMPIRE can be seamlessly adapted to multiple GNN architectures and consistently lead to significant improvement in edge prediction accuracy.

2 PRELIMINARIES

We begin by describing the formation of edge prediction and introducing the associated notations.

Definition 1. (GNN-based Edge Prediction Framework) *Considering a graph $\mathcal{G} = (\mathcal{V}, \mathcal{E})$,* where $\mathcal{V} = \{v_1, \ldots, v_N\}$ is the set of nodes and $\mathcal{E}$ is the set of edges connecting these nodes and assuming that each node v_n has a feature vector $\boldsymbol{x}_n$, the n-th row of the feature matrix $\boldsymbol{X}$, we can build an arbitrary GNN model (denoted as $\mathsf{GNN}(\cdot)$) to encode the embedding vector for each node. In other words, we have $\boldsymbol{H} = \mathsf{GNN}(\mathcal{G}, \boldsymbol{X})$, where $\boldsymbol{H}$ denotes the embedding matrix. We directly plug the learned node embeddings into a score function (denoted as $\mathsf{S}(\cdot)$) to obtain the final prediction of the edge existence of each pair nodes $\langle s, t\rangle$ (denoted as $\widehat{y}_{st}$), which can be formulated as*

$$\widehat{y}_{st} = \mathsf{S}(\mathsf{GNN}(\mathcal{G}, \boldsymbol{X})_s, \mathsf{GNN}(\mathcal{G}, \boldsymbol{X})_t). \tag{1}$$

One widely adopted loss is a log loss L defined as

$$L = -\sum_{\langle v_s, v_t\rangle \in \mathcal{V}\times\mathcal{V}} (y_{st} \log \widehat{y}_{st} + (1 - y_{st}) \log(1 - \widehat{y}_{st})), \tag{2}$$

where y_{st} is the label for node pair $\langle v_s, v_t\rangle$.

To be more specific regarding how GNN models work, we briefly review conventional message passing mechanism [4]. The message passing runs multiple rounds on graph to update the node embeddings, where the embedding vector $\boldsymbol{h}_s^{(l+1)}$ of node s in iteration $l+1$ is updated by

$$\boldsymbol{h}_s^{(l+1)} = \mathsf{U}(\boldsymbol{h}_s^{(l)}, \{\boldsymbol{m}_{s\leftarrow w}^{(l)} | w \in \mathcal{N}_{\mathcal{E}}(s)\}), \tag{3}$$

where $\mathsf{U}(\cdot)$ denotes the node embedding update function, $\boldsymbol{m}_{s\leftarrow w}^{(l)}$ denotes the message passing from v_w to v_s, generated by a message generation function. $\mathcal{N}_{\mathcal{E}}(s)$ denotes the set of neighbor nodes connecting to v_s via the edges in $\mathcal{E}$, and the initial embedding is set as $\boldsymbol{h}_s^{(0)} = \boldsymbol{x}_s$. The above framework has derived many popular variants in terms of different designs of $\mathsf{U}(\cdot)$ and $\mathsf{M}(\cdot)$ such as GCN [11], SAGE [5], GAT [22], GIN [32]. We encourage the readers to refer to [4] for detailed background.

Based on the above framework, there are several key technical details that are frequently overlooked, and yet nonetheless can play a vital role in achieving satisfactory performance:

*For simplicity, we omit the relation (i.e., the type of edges) in this paper, since it is straightforward to extend our proposed techniques across GNN backbones (e.g., GCN, GAT) into the corresponding relational GNN backbones (e.g., RGCN [18], RGAT [3]) modelling the relational data.

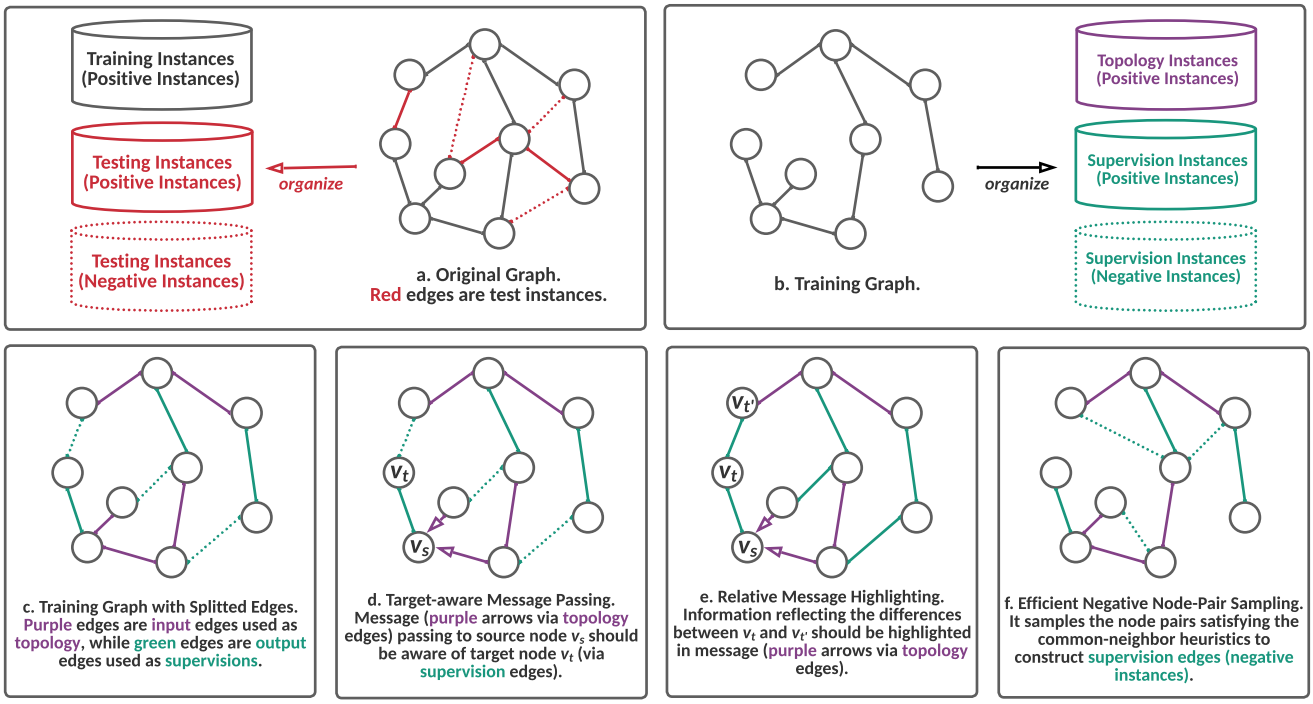

Figure 2: An illustrated example of the proposed framework EMPIRE for the edge prediction task. Given the original graph, as shown in (a), we can first remove the test edges to form the training graph, as shown in (b). Then, to align the training and test processes of the GNN models, we propose to split the training edges into the topology edges and supervision edges, as shown in (c), where each edge is used as either topology or supervision. On the basis of the splitted edges, we develop a novel target-aware passing mechanism to make the messages to the source nodes being aware of the target nodes, as shown in (d). We further highlight the relative messages that can reflect the differences between the node pairs connected by the supervision edges and those unconnected node pairs, as shown in (e). In addition, we also design a new negative node-pair sampling trick that can efficiently sample the node pairs satisfying the common-neighbor heuristics to construct the negative instances in the supervision edges, as shown in (f).

- *Whether the settings of training and test processes of the edge prediction task are aligned or not.* Given an original graph $\mathcal{G} = (\mathcal{V}, \mathcal{E})$, a principle data preprocessing procedure would first remove the test edges $\mathcal{E}_{\texttt{te}}$ from the graph is to construct a training graph $\mathcal{G}_{\texttt{tr}} = (\mathcal{V}, \mathcal{E}_{\texttt{tr}})$ (and $\mathcal{E} = \mathcal{E}_{\texttt{tr}} \cup \mathcal{E}_{\texttt{te}}$). Then, the GNN models are trained to recover $\mathcal{E}_{\texttt{tr}}$ given $\mathcal{G}_{\texttt{tr}}$ (a graph containing the edges in $\mathcal{E}_{\texttt{tr}}$); while the GNN models are evaluated to recover $\mathcal{E}_{\texttt{te}}$ given $\mathcal{G}_{\texttt{tr}}$ (a graph NOT containing the edges in $\mathcal{E}_{\texttt{te}}$). This misalignment would encourage the models to over-fit the training graph, since the training graph has already contained all the information to predict; and thus it would make the models convey the low generalizability to the test graph.
- *Whether the message passing mechanism and the prediction objective are aligned or not.* As shown in Eq. (3), the conventional message passing mechanism passes and aggregates the neighborhood information of each node v_s to update the embedding vector of v_s; while as Eq. (1) shows, the prediction objective is each pair of nodes $\langle v_s, v_t \rangle$. Therefore, previous message passing mechanism focuses on the individual node; however, the prediction objectives require it to optimize over the node pairs.

3 THE EMPIRE FRAMEWORK

3.1 Edge Splitting

To begin with, we note that the main difference between the training and test processes of the GNN models is that during the test process, each edge is used as either topology or supervision: edges in $\mathcal{E}_{\texttt{tr}}$ are used as topology and edges in $\mathcal{E}_{\texttt{te}}$ are used as supervision; while during the training process, each edge (in $\mathcal{E}_{\texttt{tr}}$) is simultaneously used as topology and supervision.

In order to align the settings of training and testing processes, we propose to specify the use of each training edge by splitting the training edges into two sets, named topology edges and supervision edges. As illustrated in Figure 2(c), the topology edges (denoted as $\mathcal{E}_{\texttt{in}}$, colored in purple) are used as the inputs to build the graph topology (i.e., to run the message passing), while the supervision edges (denoted as $\mathcal{E}_{\texttt{out}}$, colored in green) are used as the outputs to supervise the GNN models (i.e., to update the parameters). After that, we would further add several randomly sampled unconnected node pairs into the supervision instances to balance the positive and negative instances, as shown in Figure 2(b).

While practice, we typically sample the splits by randomly assigning each edge to $\mathcal{E}_{\texttt{out}}$ with some probability $\lambda \in (0, 1)$, and

the rest edges are assigned to $\mathcal{E}_{\text{in}}$. We empirically investigate the impact of λ in Section 5.3.

3.2 Target-aware Message Passing

As discussed in Section 2, in the context of conventional message passing mechanism, the representations of source and target nodes are solely determinated by their previous embedding vectors and neighbor nodes, but not being aware of each other. We argue that as the labels of the edge prediction task are on node pairs instead of nodes; and thus independently considering individual node in the message generation would lead to a sub-optimal solution.

Formally, for each source node v_s, if following conventional message passing mechanism, then the message generated from its neighbor node v_w to v_s can be formulated as $\boldsymbol{m}_{s\leftarrow w}^{(l)} = \mathtt{M}(\boldsymbol{h}_s^{(l)}, \boldsymbol{h}_w^{(l)})$.

In order to make the messages to the source node v_s being aware of the target node v_t, one straightforward approach is to generate the message following the formulation $\boldsymbol{m}_{s\leftarrow w|t}^{(l)} = \mathtt{M}(\boldsymbol{h}_s^{(l)}, \boldsymbol{h}_w^{(l)}, \boldsymbol{h}_t^{(l)})$. However, there are often a large number of target nodes for each source node, and thus it is computationally consuming or even infeasible to generate the messages for each node pair $\langle v_s, v_t \rangle$.

To make it scalable, when generating the message from neighbor node v_w to the source node v_s, we propose to model the influence of all the target nodes (i.e., v_ts) together as

$$\boldsymbol{m}_{s\leftarrow w}^{(l)} = \mathtt{M}(\boldsymbol{h}_s^{(l)}, \boldsymbol{h}_w^{(l)}, \{\boldsymbol{h}_t^{(l)} | v_t \in \mathcal{N}_{\mathcal{E}_{\text{out}}}(s)\}), \tag{4}$$

where $\mathcal{N}_{\mathcal{E}_{\text{out}}}(s)$ represents a set of the target nodes connecting to v_s by the supervision edges. With the generated message $\boldsymbol{m}_{s\leftarrow w}^{(l)}$, we then can update the representation vector $\boldsymbol{h}_s^{(l+1)}$ of each source node following

$$\boldsymbol{h}_s^{(l+1)} = \mathtt{U}(\boldsymbol{h}_s^{(l)}, \{\boldsymbol{m}_{s\leftarrow w}^{(l)} | v_w \in \mathcal{N}_{\mathcal{E}_{\text{in}}}(s)\}), \tag{5}$$

where $\mathcal{N}_{\mathcal{E}_{\text{in}}}(s)$ denotes a set of neighbor nodes connecting to v_s by the topology edges.

Notice that the designs of $\mathtt{M}(\cdot)$ also vary for different GNN architectures. For clarity, we examplify how to seamlessly adopt our approach (i.e., Eqs. (4) and (5)) into GNN models in the context of GAT model. In this case, $\mathtt{M}(\cdot)$ is implemented as

$$\boldsymbol{m}_{s\leftarrow w}^{(l)} = \alpha_{s\leftarrow w}^{(l)} \boldsymbol{h}_w^{(l)}, \tag{6}$$

where $\alpha_{s\leftarrow w}^{(l)}$ is a learnable attention weight to make the message dependent on the affinity between nodes v_s and v_w, i.e., passing more messages from the neighbor nodes similar to the source node. $\alpha_{s\leftarrow w}^{(l)}$ is computed as

$$\alpha_{s\leftarrow w}^{(l)} = \frac{\exp\left(\text{LeakyReLU}(\boldsymbol{w}^\top [\boldsymbol{h}_s^{(l)} \| \boldsymbol{h}_w^{(l)}])\right)}{\sum_{v_o \in \mathcal{N}_{\mathcal{E}_{\text{in}}}(s)} \exp\left(\text{LeakyReLU}(\boldsymbol{w}^\top [\boldsymbol{h}_s^{(l)} \| \boldsymbol{h}_o^{(l)}])\right)}, \tag{7}$$

where $\|$ represents the concatenation operation, and $\boldsymbol{w}$ is trainable vector. These messages are later used to refine the representation of the source node v_s by $\mathtt{U}(\cdot)$ (in Eq. (5)) implemented as

$$\boldsymbol{h}_s^{(l+1)} = \sigma\left(\boldsymbol{W}^{(l)} \boldsymbol{h}_s^{(l)} + \sum_{v_w \in \mathcal{N}_{\mathcal{E}_{\text{in}}}(s)} \boldsymbol{m}_{s\leftarrow w}^{(l)}\right), \tag{8}$$

where σ is an activation function, and $\boldsymbol{W}$ is the trainable matrix.

Algorithm 1: EMPIRE

INPUT: training graph $\mathcal{G}_{\mathtt{tr}} = (\mathcal{V}, \mathcal{E}_{\mathtt{tr}})$, node feature $\boldsymbol{X}$

1: **repeat**
2: Obtain $\mathcal{E}_{\mathtt{in}}, \mathcal{E}_{\mathtt{out}}$ by randomly splitting $\mathcal{E}_{\mathtt{tr}}$
3: Construct $\mathcal{D}_{\mathtt{out}}$ using Algorithm 3
4: Modify message passing function $\mathtt{M}(\cdot)$ using Eq. (9)
5: Modify update function $\mathtt{U}(\cdot)$ using Eq. (13)
6: Produce $\{\widehat{y}_{st} | \langle v_s, v_t \rangle \in \mathcal{D}_{\mathtt{out}}\}$ using Eq. (1)
7: Update parameters by minimizing L over $\mathcal{D}_{\mathtt{out}}$ in Eq. (2)
8: **until** convergence

Based on the layer-wise propagation rule of GAT introduced above, to empower the GAT with the proposed technique, we modify its $\mathtt{M}(\cdot)$ (i.e., Eq. (6)) following Eq. (4) as

$$\boldsymbol{m}_{s\leftarrow w}^{(l)} = \alpha_{s\leftarrow w}^{(l)} \left(\boldsymbol{h}_w^{(l)} + \sum_{v_t \in \mathcal{N}_{\mathcal{E}_{\text{out}}}(s)} \beta_{w|t}^{(l)} \boldsymbol{h}_w^{(l)}\right), \tag{9}$$

where $\beta_{w|t}^{(l)}$ is another learnable attention weight to mke the message aware of the target node v_t, e.g., passing more messages from the neighbor nodes related to v_t. $\beta_{w|t}^{(l)}$ is calculated as

$$\beta_{w|t}^{(l)} = \frac{\exp\left(\text{LeakyReLU}(\boldsymbol{w}^\top [\boldsymbol{h}_t^{(l)} \| \boldsymbol{h}_w^{(l)}])\right)}{\sum_{v_o \in \mathcal{N}_{\mathcal{E}_{\text{out}}}(s)} \exp\left(\text{LeakyReLU}(\boldsymbol{w}^\top [\boldsymbol{h}_w^{(l)} \| \boldsymbol{h}_o^{(l)}])\right)}. \tag{10}$$

We then feed $\boldsymbol{m}_{s\leftarrow w}^{(l)}$ computed by Eq. (9) into Eq. (8) to complete the calculation of the representation vector of v_s in iteration $l+1$.

3.3 Relative Message Highlighting

The above subsection describes the modification on the message generation function to let the messages be aware of the target nodes. We notice that after each split, there are three types of node pairs with different likelihoods of the edge existence: ones connected by the topology edges, ones connected by the supervision edges, and unconnected ones. Inspired by recent success of contrastive learning [16, 23, 42] on graphs, we consider the unconnected node pairs as the baseline node pairs. In this regard, the relative messages that can reflect the differences between the node pairs connected by the supervision edges and baseline node pairs is super informative, as it is the basis of the prediction of the edge existence.

To achieve this, we modify the update function (i.e., Eq. (5)) as

$$\boldsymbol{h}_s^{(l+1)} = \mathtt{U}(\boldsymbol{h}_s^{(l)}, \{\boldsymbol{m}_{s\leftarrow w}^{(l)}, \gamma_{s\leftarrow w}^{(l)} | v_w \in \mathcal{N}_{\mathcal{E}_{\text{in}}}(s)\}), \tag{11}$$

where $\gamma_{s\leftarrow w}^{(l)}$ is a learnable attention weight to measure the relative information in message $\boldsymbol{m}_{s\leftarrow w}^{(l)}$. $\gamma_{s\leftarrow w}^{(l)}$ is computed as

$$\gamma_{s\leftarrow w}^{(l)} = \frac{\sum_{t \in \mathcal{N}_{\mathcal{E}_{\text{out}}}(s)} \exp\left(\text{LeakyReLU}(\boldsymbol{w}^\top [\boldsymbol{h}_t^{(l)} \| \boldsymbol{m}_{s\leftarrow w}^{(l)}])\right)}{\sum_{t' \in \mathcal{B}(s)} \exp\left(\text{LeakyReLU}(\boldsymbol{w}^\top [\boldsymbol{h}_{t'}^{(l)} \| \boldsymbol{m}_{s\leftarrow w}^{(l)}])\right)}, \tag{12}$$

where $\mathcal{B}(s) \subseteq \mathcal{V} / \mathcal{N}_{\mathcal{E}_{\text{in}} \cup \mathcal{E}_{\text{out}}}(s)$ is a set of randomly sampled nodes that are unconnected to the source node v_s, and $|\mathcal{B}(s)| = |\mathcal{N}_{\mathcal{E}_{\text{out}}}(s)|$. From Eq. (12), when the message is "close" to the representation vectors of the target node and "distant" to the representation vectors of unconnected nodes, it will receive high attention.

While taking Eq. (11) into practice, we can modify Eq. (8) as

$$\boldsymbol{h}_s^{(l+1)} = \sigma\left(\boldsymbol{W}^{(l)}\boldsymbol{h}_s^{(l)} + \sum_{v_w \in \mathcal{N}_{\mathcal{E}_{\mathtt{in}}}(s)} \gamma_{s\leftarrow w}^{(l)} \boldsymbol{m}_{s\leftarrow w}^{(l)}\right). \tag{13}$$

3.4 Efficient Negative Node-Pair Sampling

As stated in Section 3.1, as Figure 2(b) depicts, EMPIRE organizes the training graph into three sets, where the topology instances and positive supervision instances are obtained from the random split; while the negative supervision instances are built by random sampling. In this subsection, we develop a new negative sampling trick regarding the generation of these negative instances.

Many recent studies especially those in the information retrieval fields such as [33, 35] reveal that introducing "hard" negative instances can improve the stability and performance of the model. There are two questions to answer for EMPIRE such that it can benefit from the "hard" negative instances: (i) what are the hard negative instances? (ii) how to efficiently sample these instances?

Regarding the edge prediction task, we define the hard negative instances as node pairs that are somewhat likely to be connected, but not connected in the training graph. Hence, a direct approach is to apply an edge prediction model over all unconnected node pairs, and select several node pairs with the high prediction scores as the hard negative instances. However, one obvious drawback of this approach is unacceptable computation costs.

To address this issue, we propose to generate the hard negative instances by using the non-parametric common-neighbor heuristic [2]. As shown in the edge prediction leaderboard[†] on Open Graph Benchmark (OGB), the common-neighbor heuristic can be regarded as a strong edge prediction model. We further develop a new retrieval algorithm to find all the node pairs containing the common neighbors with $O(|\mathcal{V}|^2)$ computations. Considering that it might be unacceptable in some real-world cases, we present an uniform sampling version to sample $n_{\mathtt{cn}}$ node pairs with $O(|\mathcal{V}|+|\mathcal{E}_{\mathtt{in}}|+n_{\mathtt{cn}})$ computations. Refer to Appendix A for the pseudo-code and analysis of these algorithms.

3.5 Model Analysis

We summarize the proposed EMPIRE paradigm in Algorithm 1, and provide the analysis of time complexity and extensions to heterogeneous graphs as follows.

Time Complexity. From Algorithm 1, we can see that there are four operations brought by EMPIRE: randomly splitting edges in line 1 costs $O(|\mathcal{E}_{\mathtt{tr}}|)$ computations, and building the supervision instances using efficient negative node-pair sampling costs $O(|\mathcal{V}|+(1+\lambda)|\mathcal{E}_{\mathtt{tr}}|)$. Let $C_{\mathtt{GNN}}$ denote the time complexity of $\mathtt{GNN}(\cdot)$. As stated in [22], GAT is computationally efficient, where the time complexity of a single GAT over F' features would be expressed as $C_{\mathtt{GNN}} = O(|\mathcal{V}|F'F+|\mathcal{E}_{\mathtt{tr}}|F')$ where F is the number of input features. Therefore, the time complexity of the target-aware message passing mechanism in line 3 is $O(|\mathcal{E}_{\mathtt{in}}||\mathcal{E}_{\mathtt{out}}|F')$, and the time complexity of the relative message highlighting in line 4 is $O(|\mathcal{V}|F'F+|\mathcal{E}_{\mathtt{out}}|F')$. The overall complexity is $O(|\mathcal{V}|F'F+|\mathcal{E}_{\mathtt{in}}||\mathcal{E}_{\mathtt{out}}|F')$.

[†]https://ogb.stanford.edu/docs/leader_linkprop/

Extension to Heterogeneous Graphs. Although we introduce EMPIRE in the context of homogeneous graphs, it is straightforward to extend it to some existing heterogeneous GNN models such as HAN [29] and RGCN [18] on heterogeneous graphs, because all these methods are developed based on the message passing mechanism. Taking HAN as an example, we provide the detailed descriptions of how to adopt EMPIRE to it in Appendix B.

We also provide the discussion on the **deployment feasibility** in Appendix D.

4 RELATED WORK

GNN Models for Edge Prediction. As GNN models have become the prevailing tool to encode the graph structure, there are an influx of works studying applying GNN models for the edge prediction task, which can be roughly categorized into two folds. One line of research [12] implicitly assumes that a GNN model holding a strong expressive power on the node representations can lead to the good link representations by combining the pair-wise node representations. For example, RGCN [18] modifies GCN [11] to encode the heterogeneity of edges (i.e., relations). Based on the assumption, one can adopt various GNN models [5, 11, 22, 30, 32, 34] original proposed for the node classification task to make the predictions of the edge existence by introducing a scoring function (also known as similarity metrics [2]). The other line of research [37, 40] implicitly assumes that subgraphs that include and do not include the edge are discriminated by the representations learned by GNN models. For instance, SEAL [37] formulates the edge prediction problems as the graph classification problems, where the models are required to classify the subgraphs including or not including the edge connecting the given node pairs. Besides these applications regarding GNN algorithms, there is an influx of literature [6, 9, 10, 28, 29, 33, 36, 38] suggesting that mining the graph structure can offer auxiliary information for recommendations. As most of the relational data (e.g., social network) in the real-world is heterogeneous, these methods pay much attention on leveraging the heterogeneity of the nodes and relations by modifying GNN architectures or introducing meta-path [21]. For example, HAN [29] adopts a hierarchical attention mechanism to capture node-level and semantic level information, which might be regarded as a heterogeneous version of GAT. All the above previous methods focus on elaborate architectures and algorithms; however, there is limited literature investigating how to adjust GNN models to make them fit the edge prediction task. We argue that it is essential, as GNN models especially those following the message passing neural network framework [4] are originally designed for the node classification task instead of the edge prediction task. In this paper, we propose a novel EMPIRE paradigm to fill the blank, which can be seamlessly incorporate with the multiple GNN models and bring significant improvements.

Simple Enhancements for GNN Models. There are several prior works [17, 30] showing that some simple modifications on GNN architectures and label usage can significantly improve the node classification accuracy. However, there are limited literature [19, 40] investigating some simple enhances regarding the edge prediction problem. From this perspective, our paper proposes some easy-to-implement refinements for apply GNN models regarding the edge prediction task, which is the first one, to our knowledge.

Table 1: Results of performance gain from different components of EMPIRE incorporating with various GNN models on the homogeneous graph datasets in terms of AUC. * indicates $p < 0.001$ in significance tests compared to Origin.

Models	Techniques	USAir	NS	PB	Yeast	C.ele	Power	Router	E.coli	Arxiv	Facebook
GCN	Origin	0.9065	0.9354	0.8963	0.9142	0.8014	0.8973	0.9034	0.9425	0.9467	0.9348
	$\text{EMPIRE}^-_{\text{split}}$	0.9248*	0.9543*	0.9177*	0.9292*	0.8220*	0.9112*	0.9278*	0.9572*	0.9533*	0.9505*
	$\text{EMPIRE}^-_{\text{+message}}$	0.9403	0.9632	0.9244	.0.9330	0.8376	0.9283	0.9346	0.9687	0.9689	0.9628
	$\text{EMPIRE}^-_{\text{+relative}}$	0.9462	0.9705	0.9336	0.9413	0.8654	0.9402	0.9583	0.9781	0.9746	0.9726
	EMPIRE	**0.9506**	**0.9797**	**0.9459**	**0.9542**	**0.8683**	**0.9420**	**0.9714**	**0.9808**	**0.9806**	**0.9747**
GIN	Origin	0.9465	0.9385	0.8911	0.9195	0.8227	0.9027	0.9104	0.9456	0.9512	0.9462
	$\text{EMPIRE}^-_{\text{split}}$	0.9650*	0.9556*	0.9098*	0.9285*	0.8343*	0.9178*	0.9275*	0.9576*	0.9656*	0.9584*
	$\text{EMPIRE}^-_{\text{+message}}$	0.9716	0.9642	0.9177	0.9274	0.8405	0.9209	0.9306	0.9606	0.9687	0.9613
	$\text{EMPIRE}^-_{\text{+relative}}$	0.9757	0.9645	0.9173	0.9283	0.8458	0.9207	0.9497	0.9688	0.9697	0.9614
	EMPIRE	**0.9765**	**0.9708**	**0.9156**	**0.9309**	**0.8467**	**0.9226**	**0.9527**	**0.9721**	**0.9702**	**0.9620**
GAT	Origin	0.9369	0.9476	0.9254	0.9395	0.8313	0.9103	0.9340	0.9422	0.9544	0.9604
	$\text{EMPIRE}^-_{\text{split}}$	0.9463*	0.9568*	0.9371*	0.9462*	0.8420*	0.9164*	0.9475*	0.9587*	0.9668*	0.9666*
	$\text{EMPIRE}^-_{\text{+message}}$	0.9597	0.9645	0.9420	0.9577	0.8482	0.9233	0.9503	0.9605	0.9689	0.9716
	$\text{EMPIRE}^-_{\text{+relative}}$	0.9576	0.9730	0.9512	0.9671	0.8441	0.9286	0.9587	0.9690	0.9697	0.9755
	EMPIRE	**0.9635**	**0.9783**	**0.9560**	**0.9685**	**0.8452**	**0.9325**	**0.9630**	**0.9727**	**0.9698**	**0.9762**
SAGE	Origin	0.9278	0.9346	0.9178	0.9235	0.8143	0.8943	0.9477	0.9436	0.9465	0.9456
	$\text{EMPIRE}^-_{\text{split}}$	0.9349*	0.9423*	0.9211*	0.9378*	0.8288*	0.9024*	0.9520*	0.9488*	0.9573*	0.9502*
	$\text{EMPIRE}^-_{\text{+message}}$	0.9466	0.9478	0.9554	0.9428	0.8345	0.9112	0.9557	0.9601	0.9608	0.9535
	$\text{EMPIRE}^-_{\text{+relative}}$	0.9487	0.9515	0.9633	0.9478	0.8403	0.9156	0.9638	0.9692	0.9682	0.9626
	EMPIRE	**0.9538**	**0.9545**	**0.9678**	**0.9492**	**0.8458**	**0.9185**	**0.9697**	**0.9715**	**0.9697**	**0.9678**

5 EXPERIMENT

5.1 Datasets and Experimental Flow

Dataset Description. To evaluate the performance of our proposed techniques, we conduct experiments on the edge prediction datasets used in [37]: **USAir** [24] is a network of US Air lines with 332 nodes and 2,126 edges. **NS** [14] is a collaboration network of researchers in network science with 1,589 nodes and 2,742 edges. **PB** [1] is a network of US political blogs with 1,222 nodes and 16,714 edges. **Yeast** [25] is a protein-protein interaction network in yeast with 2,375 nodes and 11,693 edges. **C.ele** [31] is a network of C.elegans with 297 nodes and 2,148 edges. **Power** [31] is an electrical grid of western US with 4,941 nodes and 6,594 edges. **Rounter** [20] is a router-level Internet with 5,022 nodes and 6,258 edges. **E.coli** [39] is a pairwise reaction network of metabolites in E.coli with 1,805 nodes and 14,660 edges. **Arxiv** [13] is an academic network with 18,722 nodes and 198,110 edges. **Facebook** [13] is a social network with 4,029 nodes and 88,324 edges.

We also employ four large-scale edge prediction benchmark datasets on OGB [8]: **ogbl-ppa** [8] is a protein-protein association graph with 576,289 nodes and 42,463,862 edges, where the task is to predict biologically meaningful associations between proteins. **ogbl-collab** [8] is an author collaboration graph with 235,868 nodes and 2,464,517 edges, where the task is to predict future collaborations. **ogbl-ddi** [8] is a drug-drug interaction network with 4,267 nodes and 2,402,800 edges, where each edge represents an interaction between drugs. **ogbl-citation2** [8] is a paper citation network with 2,927,963 nodes and 30,561,187 edges, where the task is to predict the missing citations.

Besides the above homogeneous graph datasets, we include four heterogeneous graph benchmark datasets: **LastFM** [7] is an audio recommendation network with 2,101 user nodes, 18,746 artist nodes, 12,648 tag nodes, 92,834 user-artist edges, 25,434 user-user edges, 186,479 user-tag edges. **Amazon** [15] is an e-commerce recommendation network with 6,170 user nodes, 2,753 item nodes, 3,857 view nodes, 334 brand nodes, 146,230 user-item edges, 5,694 item-view edges, 2,753 item-brand edges, 37,958 user-user edges. **Yelp** [7] is a business-based social network with 16,239 user nodes, 14,284 business nodes, 47 city nodes, 511 genre nodes, 198,397 user-business edges, 158,590 user-user edges, 76,875 user-city edges, 14,267 business-city edges, 40,009 business-genre edges. **Douban** [41] is a book recommendation network with 13,024 user nodes, 22,347 book nodes, 2,936 group nodes, 10,805 author nodes, 1,815 publisher nodes, 598,420 user-book edges, 169,150 user-user edges, 1,189,271 user-group edges, 21,907 book-author edges, 21,773 book-publisher edges.

We provide the detailed descriptions of data preprocessing and hyperparameter settings in Appendix C.2. We evaluate the performance in terms of Area Under ROC Curve (AUC), Accuracy (ACC), F1 score (F1). The threshold for positive prediction is set as 0.5.

Baseline Description. We note that EMPIRE can be regarded as plug-in techniques that can be seamlessly incorporate into various GNN models on both homogeneous and heterogeneous graph datasets. To be more specific, for homogeneous GNN models, we introduce the following GNN models as the basic model: **GCN** [11], **GIN** [32], **GAT** [22], **SAGE** [5]. For heterogeneous graph datasets, we use the following GNN models as the basic model: **RGCN** [18], **HAN** [29]. We provide the detailed descriptions of these baselines in Appendix C.1.

Table 2: Results of performance gain from different components of EMPIRE on the large homogeneous graph datasets in terms of AUC, ACC, F1. * in $\text{EMPIRE}^{-}_{\texttt{split}}$ indicates $p < 0.001$ in significance tests compared to Origin.

Models	Techniques	ogb-ppa			ogb-collab			ogb-ddi			ogb-citation2		
		AUC	ACC	F1	AUC	ACC	F1	AUC	ACC	F1	AUC	ACC	F1
GCN	Origin	0.9532	0.9325	0.9363	0.9609	0.9422	0.9431	0.9046	0.8887	0.8908	0.9542	0.9360	0.9382
	$\text{EMPIRE}^{-}_{\texttt{split}}$	0.9586*	0.9387*	0.9398*	0.9634*	0.9446*	0.9557*	0.9178*	0.8904*	0.8934*	0.9591*	0.9473*	0.9494*
	$\text{EMPIRE}^{-}_{\texttt{+message}}$	0.9597	0.9459	0.9411	0.9655	0.9469	0.9590	0.9195	0.8927	0.8956	0.9660	0.9579	0.9518
	$\text{EMPIRE}^{-}_{\texttt{+relative}}$	0.9619	0.9550	0.9532	0.9678	0.9497	0.9638	0.9284	0.8986	0.8994	0.9675	0.9635	0.9646
	EMPIRE	**0.9632**	**0.9564**	**0.9519**	**0.9763**	**0.9525**	**0.9681**	**0.9301**	**0.9004**	**0.9062**	**0.9725**	**0.9755**	**0.9763**
GAT	Origin	0.9213	0.8980	0.9031	0.9532	0.9351	0.9387	0.9246	0.9053	0.9074	0.9478	0.9254	0.9276
	$\text{EMPIRE}^{-}_{\texttt{split}}$	0.9341*	0.9153*	0.9187*	0.9566*	0.9387*	0.9402*	0.9358*	0.9167*	0.9196*	0.9586*	0.9361*	0.9385*
	$\text{EMPIRE}^{-}_{\texttt{+message}}$	0.9394	0.9196	0.9205	0.9592	0.9424	0.9488	0.9426	0.9218	0.9212	0.9619	0.9478	0.9493
	$\text{EMPIRE}^{-}_{\texttt{+relative}}$	0.9428	0.9227	0.9296	0.9617	0.9493	0.9489	0.9472	0.9286	0.9277	0.9623	0.9484	0.9506
	EMPIRE	**0.9477**	**0.9292**	**0.9332**	**0.9626**	**0.9519**	**0.9545**	**0.9501**	**0.9324**	**0.9355**	**0.9712**	**0.9532**	**0.9556**
SAGE	Origin	0.9083	0.8843	0.8832	0.9612	0.9453	0.9465	0.9103	0.8943	0.8965	0.9321	0.9134	0.9171
	$\text{EMPIRE}^{-}_{\texttt{split}}$	0.9224*	0.8927*	0.9001*	0.9665*	0.9477*	0.9489*	0.9242*	0.9075*	0.9092*	0.9444*	0.9256*	0.9290*
	$\text{EMPIRE}^{-}_{\texttt{+message}}$	0.9252	0.8961	0.9030	0.9694	0.9498	0.9507	0.9324	0.9113	0.9131	0.9492	0.9283	0.9305
	$\text{EMPIRE}^{-}_{\texttt{+relative}}$	0.9295	0.8980	0.9040	0.9711	0.9601	0.9523	0.9353	0.9196	0.9190	0.9548	0.9359	0.9394
	EMPIRE	**0.9316**	**0.8987**	**0.9196**	**0.9734**	**0.9624**	**0.9532**	**0.9379**	**0.9214**	**0.9214**	**0.9573**	**0.9385**	**0.9417**

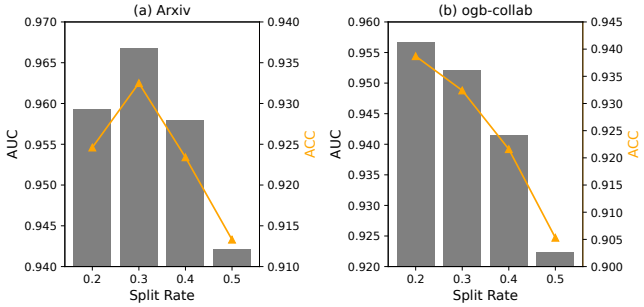

Figure 3: Comparison of performance of EMPIRE using GAT as the basic GNN model under different split rate λ on Arxiv dataset (depicted in (a)) and ogb-collab dataset (depicted in (b)) in terms of AUC and ACC.

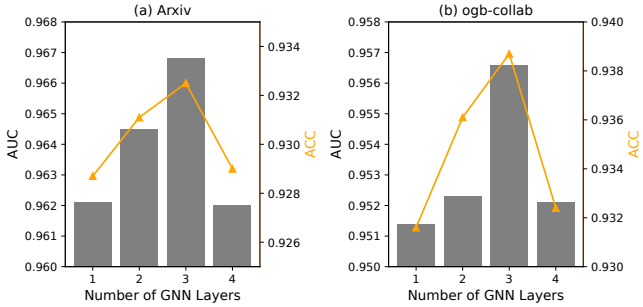

Figure 4: Comparison of performance of EMPIRE using GAT as the basic GNN model under different number of GNN layers on Arxiv dataset (depicted in (a)) and ogb-collab dataset (depicted in (b)) in terms of AUC and ACC.

Noting that the edge splitting technique is the basis of other techniques, to evaluate the performance gain from each component of EMPIRE, we construct following variants of EMPIRE:

- **Origin** directly uses the basic GNN models.
- $\textbf{EMPIRE}^{-}_{\texttt{split}}$ applies the edge splitting technique (introduced in Section 3.1) to the basic GNN models.
- $\textbf{EMPIRE}^{-}_{\texttt{+message}}$ employs the target-aware message passing mechanism (introduced in Section 3.2) to $\text{EMPIRE}^{-}_{\texttt{split}}$.
- $\textbf{EMPIRE}^{-}_{\texttt{+relative}}$ combines the relative message highlighting technique (introduced in Section 3.3) to $\text{EMPIRE}^{-}_{\texttt{+message}}$.
- **EMPIRE** applies the efficient negative node-pair sampling trick (introduced in Section 3.4) to $\text{EMPIRE}^{-}_{\texttt{+relative}}$, namely it includes all the proposed techniques.

5.2 Performance Comparison

Tables 1, 2 and 3 summarize all the main results. From tables, we can see that the performance gains from our techniques vary with different basic GNN models. We list the major findings as follows.

- Results of comparisons between Origin and $\text{EMPIRE}^{-}_{\texttt{split}}$ demonstrate the superiority of our proposed edge splitting technique, where the performance gains can be attributed to specifying use of each edge. We note that this technique is super simple yet can consistently bring the significant improvement in various graphs.
- Comparisons between $\text{EMPIRE}^{-}_{\texttt{+message}}$ and $\text{EMPIRE}^{-}_{\texttt{split}}$ show the performance gain brought from our proposed target-aware message passing mechanism. And, comparisons between $\text{EMPIRE}^{-}_{\texttt{+relative}}$ and $\text{EMPIRE}^{-}_{\texttt{+message}}$ illustrates the performance gain brought from the proposed relative message highlighting technique. Comparing to other techniques, the performance of this relative message highlighting technique is less stable. One possible explanation is that as defined in Eq. (12), it is calculated using randomly sampled nodes, which might make its performance partly rely on randomness.
- The differences between results of $\text{EMPIRE}^{-}_{\texttt{sample}}$ and EMPIRE show the performance gain from the efficient negative node-pair sampling trick. It performance gain usually might be not as significant as that of other techniques, but is very stable.

Table 3: Results of performance gain from different components of EMPIRE on the heterogeneous graph datasets in terms of AUC, ACC, F1. * in $\text{EMPIRE}^{-}_{\text{split}}$ indicates $p < 0.001$ in significance tests compared to Origin.

Models	Techniques	LastFM			Amazon			Yelp			Douban		
		AUC	ACC	F1	AUC	ACC	F1	AUC	ACC	F1	AUC	ACC	F1
RGCN	Origin	0.8532	0.8382	0.8354	0.8120	0.7403	0.7322	0.8879	0.8411	0.8330	0.9203	0.8412	0.8267
	$\text{EMPIRE}^{-}_{\text{split}}$	0.8624*	0.8447*	0.8412*	0.8125*	0.7496*	0.7346*	0.8935*	0.8504*	0.8434*	0.9351*	0.8573*	0.8394*
	$\text{EMPIRE}^{-}_{\text{+message}}$	0.8697	0.8459	0.8511	0.8155	0.7529	0.7490	0.9095	0.8527	0.8456	0.9380	0.8589	0.8428
	$\text{EMPIRE}^{-}_{\text{+relative}}$	0.8719	0.8550	0.8552	0.8208	0.7557	0.7512	0.9144	0.8616	0.8494	0.9455	0.8645	0.8496
	EMPIRE	**0.8732**	**0.8564**	**0.8591**	**0.8263**	**0.7575**	**0.7581**	**0.9181**	**0.8684**	**0.8562**	**0.9565**	**0.8695**	**0.8533**
HAN	Origin	0.8915	0.8336	0.8296	0.9156	0.8488	0.8427	0.8487	0.7682	0.7572	0.9243	0.8500	0.8451
	$\text{EMPIRE}^{-}_{\text{split}}$	0.9086*	0.8417*	0.8358*	0.9234*	0.8525*	0.8496*	0.8527*	0.7753*	0.7625*	0.9286*	0.8586*	0.8488*
	$\text{EMPIRE}^{-}_{\text{+message}}$	0.9127	0.8464	0.8395	0.9264	0.8587	0.8568	0.8616	0.7812	0.7723	0.9313	0.8603	0.8556
	$\text{EMPIRE}^{-}_{\text{+relative}}$	0.9183	0.8523	0.8435	0.9310	0.8621	0.8598	0.8677	0.7865	0.7786	0.9376	0.8665	0.8611
	EMPIRE	**0.9194**	**0.8535**	**0.8472**	**0.9356**	**0.8654**	**0.8623**	**0.8714**	**0.7935**	**0.7842**	**0.9463**	**0.8732**	**0.8642**

5.3 Impact of Split Rate

As our edge splitting technique is the basis of all other techniques, thus it is essential to investigate the impact of split rate λ. From the description in Section 3.1, when λ approaches zero, there is no edge used as the supervisions which is meaningless; while when λ tends to one, it represents the case where there is no input graph topology which also tells nothing. Hence, we select 0.2, 0.3, 0.4, 0.5 as the values of λ to depict the trend in term of AUC and ACC on Arxiv and ogb-collab datasets. As Figure 3 shows, the best performance often occurs around 0.2 to 0.3, showing that 70% to 80% edges used as the topology and the rest 30% to 20% edges used as the supervisions mgiht be the best choice in most best cases. One possible reason is that a larger λ means more edges used as the supervisions and less edges used for the topology, which would cause the data sparsity issue on the input graph; while a smaller λ would encourage the model to focus more on the input graph, which might lead to the over-fitting issue.

5.4 Impact of Number of GNN Layers

Another key hyperparameter is the number of layers of GNN models. Normally speaking, the best choice of the number of GNN layers are among the values 1,2,3,4. Therefore, we evaluate their performance in term of AUC and ACC on Arxiv and ogb-collab datasets and depict the results in Figure 4, which shows the performance changes from the number of GNN layers are relatively small, and among those choices 3 might be the best one in the most cases.

5.5 Time Complexity

We study the time complexity of applying the proposed technique on Arxiv dataset, and depict the training and inference times for one round of the whole data in Figure 5. From the figure, our efficient negative node-pair sampling algorithm still consume much time during training. To solve this, one possible solution is to precompute and store these node pairs into buffer, and then we can simply sample instances from the buffer during training. We also note that there is almost no extra cost for inference time.

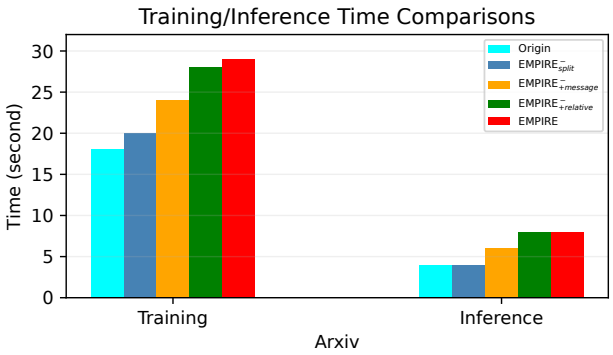

Figure 5: Comparisons of training and inference time of EMPIRE and its variants using GAT as the basic GNN model on Arxiv dataset.

6 CONCLUSION AND FUTURE WORK

In this paper, we first analyze the key differences between the node classification and edge prediction tasks, and present a novel GNN based edge prediction framework named EMPIRE to tailor existing GNN models (originally proposed for the node classification task) to be more fit for the edge prediction task. Specifically, we first propose to specify the edge usage to avoid the models over-fitting the training graph, and then develop a novel target-aware message passing mechanism to make the messages to the source nodes be aware of the target nodes. In addition, we also show that highlighting relative message and sampling hard negative instances could further improve the performance. Our experimental results demonstrate that our techniques can be applied to various GNN models. Future work could focus on incorporating them into other graph tasks (e.g., graph classification).

REFERENCES

[1] Robert Ackland et al. 2005. Mapping the US political blogosphere: Are conservative bloggers more prominent?. In *BlogTalk Downunder 2005 Conference, Sydney*.

[2] Lada A Adamic and Eytan Adar. 2003. Friends and neighbors on the web. *Social networks* (2003).

[3] Dan Busbridge, Dane Sherburn, Pietro Cavallo, and Nils Y Hammerla. 2019. Relational graph attention networks. *Technical report arXiv:1904.05811* (2019).

[4] Justin Gilmer, Samuel S Schoenholz, Patrick F Riley, Oriol Vinyals, and George E Dahl. 2017. Neural message passing for quantum chemistry. In *ICML*.

[5] William L Hamilton, Rex Ying, and Jure Leskovec. 2017. Inductive representation learning on large graphs. In *NIPS*.

[6] Xiangnan He, Kuan Deng, Xiang Wang, Yan Li, Yongdong Zhang, and Meng Wang. 2020. Lightgcn: Simplifying and powering graph convolution network for recommendation. In *SIGIR*.

[7] Binbin Hu, Chuan Shi, Wayne Xin Zhao, and Tianchi Yang. 2018. Local and global information fusion for top-n recommendation in heterogeneous information network. In *CIKM*.

[8] Weihua Hu, Matthias Fey, Marinka Zitnik, Yuxiao Dong, Hongyu Ren, Bowen Liu, Michele Catasta, and Jure Leskovec. 2020. Open graph benchmark: Datasets for machine learning on graphs. In *Technical report arXiv:2005.00687*.

[9] Ziniu Hu, Yuxiao Dong, Kuansan Wang, and Yizhou Sun. 2020. Heterogeneous graph transformer. In *WWW*.

[10] Jiarui Jin, Jiarui Qin, Yuchen Fang, Kounianhua Du, Weinan Zhang, Yong Yu, Zheng Zhang, and Alexander J Smola. 2020. An efficient neighborhood-based interaction model for recommendation on heterogeneous graph. In *KDD*.

[11] Thomas N Kipf and Max Welling. 2016. Semi-supervised classification with graph convolutional networks. In *ICLR*.

[12] Thomas N Kipf and Max Welling. 2016. Variational graph auto-encoders. *Technical report arXiv:1611.07308* (2016).

[13] Jure Leskovec and Andrej Krevl. 2015. *SNAP Datasets:Stanford large network dataset collection*. (2015).

[14] Mark EJ Newman. 2006. Finding community structure in networks using the eigenvectors of matrices. *Physical review E* (2006).

[15] Jianmo Ni, Jiacheng Li, and Julian McAuley. 2019. Justifying recommendations using distantly-labeled reviews and fine-grained aspects. In *EMNLP*.

[16] Jiezhong Qiu, Qibin Chen, Yuxiao Dong, Jing Zhang, Hongxia Yang, Ming Ding, Kuansan Wang, and Jie Tang. 2020. Gcc: Graph contrastive coding for graph neural network pre-training. In *KDD*.

[17] Yu Rong, Wenbing Huang, Tingyang Xu, and Junzhou Huang. 2019. Dropedge: Towards deep graph convolutional networks on node classification. *ICLR* (2019).

[18] Michael Schlichtkrull, Thomas N Kipf, Peter Bloem, Rianne Van Den Berg, Ivan Titov, and Max Welling. 2018. Modeling relational data with graph convolutional networks. In *ESWC*.

[19] Abhay Singh, Qian Huang, Sijia Linda Huang, Omkar Bhalerao, Horace He, Ser-Nam Lim, and Austin R Benson. 2021. Edge proposal sets for link prediction. *Technical report arXiv:2106.15810* (2021).

[20] Neil Spring, Ratul Mahajan, and David Wetherall. 2002. Measuring ISP topologies with Rocketfuel. *ACM SIGCOMM Computer Communication Review* (2002).

[21] Yizhou Sun, Jiawei Han, Xifeng Yan, Philip S Yu, and Tianyi Wu. 2011. Pathsim: Meta path-based top-k similarity search in heterogeneous information networks. *Proceedings of the VLDB Endowment* (2011).

[22] Petar Veličković, Guillem Cucurull, Arantxa Casanova, Adriana Romero, Pietro Lio, and Yoshua Bengio. 2018. Graph attention networks. In *ICLR*.

[23] Petar Velickovic, William Fedus, William L Hamilton, Pietro Liò, Yoshua Bengio, and R Devon Hjelm. 2019. Deep Graph Infomax. *ICLR* (2019).

[24] Andrej Mrvar Vladimir Batagelj. 2006. *http://vlado.fmf.uni-lj.si/pub/networks/data/* (2006).

[25] Christian Von Mering, Roland Krause, Berend Snel, Michael Cornell, Stephen G Oliver, Stanley Fields, and Peer Bork. 2002. Comparative assessment of large-scale data sets of protein–protein interactions. *Nature* (2002).

[26] Alastair J Walker. 1977. An efficient method for generating discrete random variables with general distributions. *TOMS* (1977).

[27] Minjie Wang, Lingfan Yu, Da Zheng, Quan Gan, Yu Gai, Zihao Ye, Mufei Li, Jinjing Zhou, Qi Huang, Chao Ma, et al. 2019. Deep Graph Library: Towards Efficient and Scalable Deep Learning on Graphs. *Technical report* (2019).

[28] Xiang Wang, Xiangnan He, Meng Wang, Fuli Feng, and Tat-Seng Chua. 2019. Neural graph collaborative filtering. In *SIGIR*.

[29] Xiao Wang, Houye Ji, Chuan Shi, Bai Wang, Yanfang Ye, Peng Cui, and Philip S Yu. 2019. Heterogeneous graph attention network. In *WWW*.

[30] Yangkun Wang, Jiarui Jin, Weinan Zhang, Yong Yu, Zheng Zhang, and David Wipf. 2021. Bag of Tricks for Node Classification with Graph Neural Networks. *DLG-KDD* (2021).

[31] Duncan J Watts and Steven H Strogatz. 1998. Collective dynamics of 'small-world'networks. *nature* (1998).

[32] Keyulu Xu, Weihua Hu, Jure Leskovec, and Stefanie Jegelka. 2018. How powerful are graph neural networks? *ICLR* (2018).

[33] Rex Ying, Ruining He, Kaifeng Chen, Pong Eksombatchai, William L Hamilton, and Jure Leskovec. 2018. Graph convolutional neural networks for web-scale recommender systems. In *KDD*.

[34] Jiaxuan You, Rex Ying, and Jure Leskovec. 2019. Position-aware graph neural networks. In *ICML*.

[35] Jingtao Zhan, Jiaxin Mao, Yiqun Liu, Jiafeng Guo, Min Zhang, and Shaoping Ma. 2021. Optimizing dense retrieval model training with hard negatives. In *SIGIR*.

[36] Chuxu Zhang, Dongjin Song, Chao Huang, Ananthram Swami, and Nitesh V Chawla. 2019. Heterogeneous graph neural network. In *KDD*.

[37] Muhan Zhang and Yixin Chen. 2018. Link prediction based on graph neural networks. *NIPS* (2018).

[38] Muhan Zhang and Yixin Chen. 2019. Inductive matrix completion based on graph neural networks. *ICLR* (2019).

[39] Muhan Zhang, Zhicheng Cui, Shali Jiang, and Yixin Chen. 2018. Beyond link prediction: Predicting hyperlinks in adjacency space. In *AAAI*.

[40] Muhan Zhang, Pan Li, Yinglong Xia, Kai Wang, and Long Jin. 2020. Revisiting graph neural networks for link prediction. *Technical report arXiv:2010.16103* (2020).

[41] Jing Zheng, Jian Liu, Chuan Shi, Fuzhen Zhuang, Jingzhi Li, and Bin Wu. 2017. Recommendation in heterogeneous information network via dual similarity regularization. *International Journal of Data Science and Analytics* (2017).

[42] Yanqiao Zhu, Yichen Xu, Feng Yu, Qiang Liu, Shu Wu, and Liang Wang. 2021. Graph contrastive learning with adaptive augmentation. In *WWW*.

A COMMON NEIGHBOR NODES RETRIEVAL AND SAMPLING ALGORITHMS

In this part, we first provide a retrieval algorithm that can search and retrieve all the node pairs satisfying the common-neighbor heuristics [2] in the training graph $\mathcal{G}_{\mathtt{tr}}$. Equivalently, we formulate the task as to find all the two-node paths in $\mathcal{G}_{\mathtt{tr}}$. Formally, our input is $\mathcal{G}_{\mathtt{tr}} = (\mathcal{V}, \mathcal{E}_{\mathtt{tr}})$ and the output is $\mathcal{B}$ containing all the node pairs.

Algorithm 2: Common Neighbor Nodes Retrieval

```
B ← {}
for each v_u ∈ V do
    for each v_o, v_w ∈ N_{E_tr}(u) do
        if ⟨v_o, v_w⟩ ∉ E_tr then
            B ← B ∪ {(v_o, v_w)}
        end
    end
end
```

Based on Algorithm 2, we can see all the unconnected node pairs (v_o, v_w) sharing the neighbor node v_u are enumerated. As the nodes v_u, v_o, v_w can be any nodes in $\mathcal{G}_{\mathtt{tr}}$, the time complexity of Algorithm 2 is $O(|\mathcal{V}|^2)$.

However, in the real-world scenarios, there are the many cases with large graphs, where Algorithm 2 might be not practical due to its high computation costs. Therefore, we further propose a novel common neighbor nodes sampling algorithm in Algorithm 3 that can uniformly sample $n_{\mathtt{cn}}$ node pairs. Its inputs and outputs are identical to Algorithm 2. Let d_u denote the degree of node v_u.

For the correctness of Algorithm 3, we formulate the sampling the node pairs into uniformly sampling three-node path, namely (v_o, v_u, v_w). We first sample the intermediate node of the path (i.e., v_u) where there are $d_u(d_u - 1)/2$ three-node paths with v_u as its intermediate node. Next, we sample v_u with the probability p_u to ensure uniformity, where $p_u = d_u(d_u - 1)/\sum_u d_u(d_u - 1)$, and then sample its two neighbor nodes to form the paths.

For the time complexity, the computation for the degree requires $O(|\mathcal{E}_{\mathtt{tr}}|)$, the first two loops require $O(|\mathcal{V}|)$, and the last loop

Algorithm 3: Common Neighbor Nodes Sampling

$\mathcal{B} \leftarrow \{\}$
for *each* $v_u \in \mathcal{V}$ **do**
  $c_u \leftarrow d_u(d_u - 1)$ where d_u is the degree of node v_u
end
$c \leftarrow \sum_u c_u$
for *each* $v_u \in \mathcal{V}$ **do**
  $p_u \leftarrow c_u / c$
end
for $i \leftarrow 1$ to n_{cn} **do**
  Sample v_u with probability p_u
  Uniformly sample two different neighbor nodes (i.e., v_o and v_w) of v_u
  if $\langle v_o, v_w \rangle \notin \mathcal{E}_{\mathsf{tr}}$ **then**
    $\mathcal{B} \leftarrow \mathcal{B} \cup \{(v_o, v_w)\}$
  end
end

requires $O(n_{\mathsf{cn}})$ if we sample (v_o, v_w) using alias method [26]. So, the overall time complexity of Algorithm 3 is $O(|\mathcal{V}| + |\mathcal{E}_{\mathsf{tr}}| + n_{\mathsf{cn}})$.

B EXTENSION TO HETEROGENEOUS GRAPHS

Previously, we have introduced EMPIRE in the context of homogeneous graphs, and exemplify our target-aware message passing and relative message highlighting techniques by GAT [22].

In this section, we describe how to extend EMPIRE to heterogeneous graphs. We first introduce the concept of heterogeneous graphs as follows. A heterogeneous graph, denoted as $\mathcal{G} = (\mathcal{V}, \mathcal{E})$, consists of a node set $\mathcal{V}$ and an edge set $\mathcal{E}$. $\mathcal{G}$ is also associated with a node type mapping function $\varphi : \mathcal{V} \rightarrow \mathcal{A}$ and an edge type mapping function $\psi : \mathcal{E} \rightarrow \mathcal{R}$. $\mathcal{A}$ and $\mathcal{R}$ are the sets of pre-defined node types and edge types, where $|\mathcal{A}| + |\mathcal{R}| > 2$.

As there are multiple types of edges, two nodes can be connected via different meta-paths which is defined as follows. A meta-path Φ is defined as a path in the form of $A_1 \xrightarrow{R_1} A_2 \xrightarrow{R_2} \cdots \xrightarrow{R_l} A_{l+1}$ that describes a composite relation $R = R_1 \odot R_2 \odot \cdots \odot R_l$ between node type A_1 and A_l and $\odot$ denotes the composition operator on the edge types. Based on a meta-path Φ, we further present the definition of the meta-path based neighborhood $\mathcal{N}_{\mathcal{E}}^{\Phi}(s)$ of node v_s as: the set of nodes which connect with node v_s via meta-path Φ.

Notice that we summarize the main techniques of EMPIRE as line 1 to line 4 in Algorithm 1. It is trivial for applying lines 1 and 2 on heterogeneous graphs. For lines 3 and 4, we further exemplify these operations with HAN [29], which can be regarded as a heterogeneous version of GAT. Concretely, we tailor Eq. (9) as

$$\boldsymbol{m}_{s\leftarrow w}^{\Phi(l)} = \alpha_{s\leftarrow w}^{\Phi(l)} \left(\boldsymbol{h}_w^{(l)} + \sum_{v_t \in \mathcal{N}_{\mathcal{E}_{\mathsf{out}}}^{\Phi}(s)} \beta_{w|t}^{\Phi(l)} \boldsymbol{h}_w^{(l)} \right), \tag{14}$$

where $\alpha_{s\leftarrow w}^{\Phi(l)}$ and $\beta_{w|t}^{\Phi(l)}$ are derived by replacing $\mathcal{N}_{\mathcal{E}}$ with $\mathcal{N}_{\mathcal{E}}^{\Phi}$ in Eqs. (7) and (10). Then, as stated in [29], these messages will be fed into a semantic-level attention to aggregate the messages passed through various meta-paths. More specifically, we tailor Eq. (13) as

$$\boldsymbol{h}_s^{(l+1)} = \sigma \left(\sum_{\Phi} \zeta^{\Phi(l)} (\boldsymbol{W}^{(l)} \boldsymbol{h}_s^{(l)} + \boldsymbol{m}_s^{\Phi(l)}) \right), \tag{15}$$

where $\boldsymbol{m}_s^{\Phi(l)}$ is the message to node v_s through meta-path Φ which can be derived as

$$\boldsymbol{m}_s^{\Phi(l)} = \sum_{v_w \in \mathcal{N}_{\mathcal{E}_{\mathsf{in}}}^{\Phi}(s)} \gamma_{s\leftarrow w}^{\Phi(l)} \boldsymbol{m}_{s\leftarrow w}^{\Phi(l)}. \tag{16}$$

Here, $\boldsymbol{m}_{s\leftarrow w}^{\Phi(l)}$ can be obtained from Eq. (14) and $\gamma_{s\leftarrow w}^{\Phi(l)}$ is calculated by replacing $\mathcal{N}_{\mathcal{E}}$ with $\mathcal{N}_{\mathcal{E}}^{\Phi}$ in Eq. (12). To obtain $\zeta^{\Phi(l)}$ in Eq. (15), we first calculate the importance of each meta-path following

$$w^{\Phi(l)} = \frac{1}{|\mathcal{V}|} \sum_{v_s \in \mathcal{V}} \boldsymbol{w}^{(l)\top} \tanh(\boldsymbol{W}^{(l)} \boldsymbol{m}_s^{\Phi(l)} + \boldsymbol{b}^{(l)}), \tag{17}$$

where $\boldsymbol{m}_s^{\Phi(l)}$ can be obtained from Eq. (16).

The attention weight of meta-path Φ denoted as $\zeta^{\Phi(l)}$, can be computed by normalizing the above importance over all the meta-paths using a softmax function as

$$\zeta^{\Phi} = \frac{\exp(w^{\Phi})}{\sum_{\Phi} \exp(w^{\Phi})}. \tag{18}$$

C EXPERIMENTS

C.1 Baseline Description

Our EMPIRE introduced in Section 3 can be regarded as plug-in techniques that can be seamlessly incorporate into various GNN models on both homogeneous and heterogeneous graph dataset. To be more specific, for homogeneous GNN models, we introduce the following GNN models as the basic model:

- **GCN** [11] is a graph convolutional network particularly designed for graph structured data.
- **GIN** [32] combines MLP with GCN that is provably as powerful as the Weisfeiler-Lehman graph isomorphism test.
- **GAT** [22] combines an attention mechanism with GCN to model the different contributions from neighbor nodes.
- **SAGE** [5] is a graph neural network following a sample-aggregation paradigm.

For heterogeneous graph datasets, we use the following GNN models as the basic model:

- **RGCN** [18] combines graph neural networks with factorization models for edge prediction task.
- **HAN** [29] is a hierarchical attention network designed on heterogeneous graphs to capture node- and semantic-level information.

C.2 Experimental Setting

For the datasets introduced in Section 5.1, we randomly split the edges into training, testing sets with the ratio of 8:2. We note that we do not directly use the splitted sets in OGB [8], as some of splits consider other factors (e.g., date information in ogbl-collab). And, our data preprocessing is also different from [37] where they randomly select 10% existing edges from each dataset as positive testing data, and use the remaining 90% existing edges for training, which forms one of important reasons for inconsistent results between Table 1 and the numbers reported in [37].

For the basic GNN methods, we employ these baseline methods based on Deep Graph Library (DGL) [27] following their original setting or directly using their official implementations. We further specify the hyper-parameter settings as follows. All the models involving GNN layers are set to have the same three layers. We fix the configurations across all the experiments, where the dimension size of the embeddings is set to 128, and the learning rate space is $[0.001, 0.0001]$. The dropout rate of input is set to 0.6, of edge is set to 0.3. We use the Adam optimizer for all the models. The models are trained under the same hardware settings with an Amazon EC2 p3.8×large instance[‡], where the GPU processor is NVIDIA Tesla V100 processor and the CPU processor is Intel Xeon E5-2686 v4 (Broadwell) processor.

D DEPLOYMENT FEASIBILITY

Here, we discuss the feasibility of industrial deployment of EMPIRE framework. As graphs (especially heterogeneous graphs) have been leveraged as powerful data organizing tools to fuse complex information and successfully applied to many information retrieval scenarios. Among them, one prevailing web-scale application of GNN models is PinSage [33]. Hence, we mainly discuss the deployment feasibility based on Pinsage.

Algorithm 4: Localized EMPIRE Convolution

INPUT: current embedding $\boldsymbol{h}_s$ for node v_s, set of neighbor embeddings via topology edges $\{\boldsymbol{h}_t | v_t \in \mathcal{N}_{\mathcal{E}_{\text{in}}}(s)\}$, set of neighbor embeddings via supervision edges $\{\boldsymbol{h}_t | v_t \in \mathcal{N}_{\mathcal{E}_{\text{out}}}(s)\}$, symmetric vector function $\mathsf{V}(\cdot)$

OUTPUT: new embedding $\boldsymbol{h}_s^{\text{new}}$ for node v_s

1: $\boldsymbol{\alpha} \leftarrow$Eq. (7), $\boldsymbol{\beta} \leftarrow$Eq. (10), $\boldsymbol{\gamma} \leftarrow$Eq. (12)
2: $\boldsymbol{n}_s \leftarrow \mathsf{V}(\{\text{ReLU}(\boldsymbol{Q}\boldsymbol{h}_s + \boldsymbol{q} | v_s \in \mathcal{N}_{\mathcal{E}_{\text{in}}}(s))\}; \boldsymbol{\alpha}, \boldsymbol{\beta})$
3: $\boldsymbol{h}_s^{\text{new}} \leftarrow \text{ReLU}(\boldsymbol{W}[\boldsymbol{h}_s, \boldsymbol{\gamma}^\top \boldsymbol{n}_s] + \boldsymbol{w})$
4: $\boldsymbol{h}_s^{\text{new}} \leftarrow \boldsymbol{h}_s^{\text{new}} / \|\boldsymbol{h}_s^{\text{new}}\|_2$

First, it is not difficult to switch the current model pipeline to EMPIRE. As stated in [33], the core of a PinSage is a localized convolution, which formulates how to aggregate information from v_s's neighborhood. To apply EMPIRE to PinSage, we modify Algorithm 1 in [33] to get the localized version of EMPIRE convolution. As shown in Algorithm 4, the main changes brought from EMPIRE are the neighbor and message weights $\boldsymbol{\alpha}$, $\boldsymbol{\beta}$, $\boldsymbol{\gamma}$ in line 1.

Second, efficiency is another essential concerns in the industrial applications. The overall complexity of EMPIRE is theoretically analyzed in Section 3.5 and empirically studied in Section 5.5. To save the computation costs, we can compute and store the weights in line 1 in an asynchronous manner. In other words, after assigning initial values to $\boldsymbol{\alpha}$, $\boldsymbol{\beta}$, $\boldsymbol{\gamma}$, we can run line 2 to line 4 for each step, but run line 1 for each T step, where T is the update interval for these weights. Or, we can also simply use the randomized learnable weights (similar to $\boldsymbol{Q}$, $\boldsymbol{q}$,$\boldsymbol{W}$,$\boldsymbol{w}$ in the algorithm) to replace $\boldsymbol{\alpha}$, $\boldsymbol{\beta}$, $\boldsymbol{\gamma}$ defined in Eqs. (7), (10), (12).

Third, from perspective of the system load, EMPIRE mainly operates the message passing mechanism during the training procedure; therefore, it is no additional cost during the inference procedure.

[‡]Detailed setting of AWS E2 instance can be found at https://aws.amazon.com/ec2/instance-types/?nc1=h_ls.